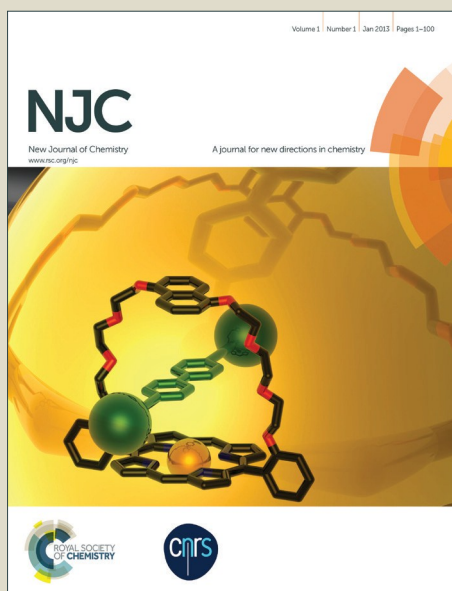


NJC

Accepted Manuscript



This is an *Accepted Manuscript*, which has been through the Royal Society of Chemistry peer review process and has been accepted for publication.

Accepted Manuscripts are published online shortly after acceptance, before technical editing, formatting and proof reading. Using this free service, authors can make their results available to the community, in citable form, before we publish the edited article. We will replace this *Accepted Manuscript* with the edited and formatted *Advance Article* as soon as it is available.

You can find more information about *Accepted Manuscripts* in the [Information for Authors](#).

Please note that technical editing may introduce minor changes to the text and/or graphics, which may alter content. The journal's standard [Terms & Conditions](#) and the [Ethical guidelines](#) still apply. In no event shall the Royal Society of Chemistry be held responsible for any errors or omissions in this *Accepted Manuscript* or any consequences arising from the use of any information it contains.

Silver(I)-based Energetic Coordination Polymers: Synthesis, Structure and Energy Performance

Xiaoni Qu, Sheng Zhang, Qi Yang, Zhiyong Su, Qing Wei,^{*} Gang Xie, Sanping Chen^{*}

^a *Key Laboratory of Synthetic and Natural Functional Molecule Chemistry of Ministry of Education, College of Chemistry and Materials Science, Northwest University, Xi'an 710069, China.*

***Corresponding author**

Prof. Sanping Chen

Tel.: +8602988302604

Fax: +8602988302604

E-mail: sanpingchen@126.com

Abstract

In this contribution two energetic coordination polymers, $[\text{Ag}(\text{atz})]_n$ (**1**) and $[\text{Ag}(\text{ntz})]_n$ (**2**) (Hatz = 3-amine-1H-1,2,4-triazole, Hntz = 3-nitro-1H-1,2,4-triazole), have been synthesized and structurally characterized. Crystal structure analyses reveal that the titled compounds possess two-dimensional (2D) three-connected layers featuring six-membered rings and sixteen-membered rings. Depend on the reaction temperature and the reactant molar ratio, the two compounds with smaller size have been prepared and their morphologies were studied. Additionally, solid-state photoluminescence for **1** and **2** at room temperature has been investigated. Noteworthy, the physicochemical property shows that **1** and **2** perform excellent insensitivity and high decomposition temperatures ($T_{\text{dec}} = 348\text{ }^{\circ}\text{C}$ for **1**, $T_{\text{dec}} = 305\text{ }^{\circ}\text{C}$ for **2**). The present research reveals that the substituent NH_2/NO_2 play a crucial role in the performances of energetic materials.

Key words: Energetic coordination polymer / Detonation performance / Morphology

Introduction

The development of energetic materials, especially high-energy-density materials (HEDM),^[1-6] has been becoming an attractive research field and great progress has been achieved.^[7-12] Taking the known conflict of high energy and insensitivity of energetic materials into consideration, thereby yielding the energetic materials with safety and high energy is still the crucial challenge in the area of energetic materials.^[13-17]

In recent years, metal organic frameworks (MOFs) have attracted considerable interest in the area of coordination chemistry and material chemistry on the basis of the following advantages: firstly, the well ordered distribution of atoms in MOFs results in the inherently structural stability and high mechanical strength;^[18] secondly, MOFs possess intriguing variety of architectures and topologies on the geometry.^[19] Predictably, the rational design and synthesis of energetic MOFs generated by metal ions and organic nitrogen-rich ligands, has been proved to be one of the optimal approaches to meeting the simultaneous requirements of high thermal stability and high heat of detonation.^[20,21]

Undoubtably, the nitrogen-rich heterocycles, particularly triazole, tetrazole and their derivatives, have been a kind of the most favoured ligands to construct high-energy-density MOFs due to their various coordination modes, inherently energetic N–N, N=N, C–N and C=N bonds and structural stability. To the best of our knowledge, a lot of excellent works have been reported. For example, Shreeve *et al.*^[22] reported two energetic metal complexes based on 5-(1-methylhydrazinyl)-tetrazolate, exhibiting promising properties in stability, sensitivity and energetic aspects. Subsequently, Pang and co-workers^[23] applied 4,4'-azo-1,2,4-triazole as ligand and synthesized two three-dimensional (3D), high-energetic MOFs featuring high detonation performances. Recently, our group^[24] synthesized two energetic MOFs with 3-(tetrazol-5-yl) triazole as ligand, which could improve the development of MOFs in the field of energetic materials. However, the different substituents on nitrogen-rich heterocycles may play a significant role in the structures and applications of energetic MOFs. In 2014, Klapötke *et al.*^[25] used 1,2-di(1H-tetrazol-5-yl) ethane and its derivative, 1,2-bis(1-methyltetrazol-5-yl) ethane, to prepare energetic copper(II) complexes, which may offer an idea to produce highly photosensitive explosives. Consequently, it has attracted our great attention that further exploring the influence of different energetic substituents of nitrogen-rich heterocycles on the structures and properties of

energetic materials.

In our recent work, 1,2,4-triazole substituted by NH_2/NO_2 , where the substituents are both energetic groups, acted as the target ligand. In addition, considering the high densities and high heats of detonation of energetic materials, we employed silver(I) with coordination diversity and flexibility as the metal ion to construct energetic MOFs with perfect detonation performances.^[26-30] It is worthy to note that our main interest is how NH_2/NO_2 substituents of 1,2,4-triazole are effective to influence the structures, photoluminescence properties and explosive performances of Ag-based coordination polymers. As expected, two energetic Ag-based coordination polymers, $[\text{Ag}(\text{atz})]_n$ (**1**) and $[\text{Ag}(\text{ntz})]_n$ (**2**), were successfully synthesized and fully characterized. Structural analyses disclose that compounds **1** and **2** feature two-dimensional (2D) three-connected layers. Significantly, we prepared the two compounds with smaller size by changing the reaction conditions and their morphologies were successfully studied by employing scanning electron microscopy. In addition, solid-state photoluminescence of **1** and **2** were also measured and discussed at room temperature. Moreover, **1** and **2** exhibit fantastic insensitivity and thermostability up to 300 °C. The detonation results were predicted by a new empirical method without depending on sophisticated computer programs previously reported by Pang *et al.*^[31]

Results and discussion

Structural description and morphological study

Crystal structure of 1: The single crystal X-ray diffraction study reveals that compound **1** crystallizes in the monoclinic $C 2/c$ space group with an asymmetric unit consisting of one crystallographically independent Ag^{I} center and one completely deprotonated atz anion, and there is no solvent molecule in this structure. Similar geometry and 2D three-connected planar layer were also identified in previously reported Ag-based compounds.^[30] As can be shown from Figure 1a, Ag^{I} center lies in a trigonal geometry, which is constituted with three nitrogen atoms from three different atz anions. And each atz anion adopts a μ_3 -1,2,4 coordination mode to bridge three Ag^{I} ions. The distances of Ag-N bonds are in the range of 2.212(3)-2.269(4) Å, and the corresponding N-Ag-N angles range from 108.07(13)° to 126.86(13)°, which are comparable to previously reported works.^[30, 31] It is worth noticing that Ag^{I} ion and atz anion as three-connected nodes are linking each other to feature six-membered rings of Ag_2N_4 units and sixteen-membered

rings of $\text{Ag}_4\text{N}_8\text{C}_4$ units, further extending into a 2D planar layer (Figures 1b and 1c). Additionally, the sixteen-membered rings are filled up with two amino units from two atz anions, and the Ag-Ag bond length in six-membered rings (Ag_2N_4) is 3.9993(6) Å. The shortest Ag-Ag distance between the adjacent layers is 3.4629(7) Å, which is well close to the sum of the van der Waals radii of two silver atoms (3.44 Å).^[27, 31] X-ray crystallography analysis determines that the shortest centroid-centroid distance of triazole rings between the adjacent layers is 3.5829(6) Å, the π - π overlap interactions between triazole rings in the neighboring layers (Supporting Information, Figure S3(a)) give rise to a 3D supramolecular framework (Figures 1d and 1e).

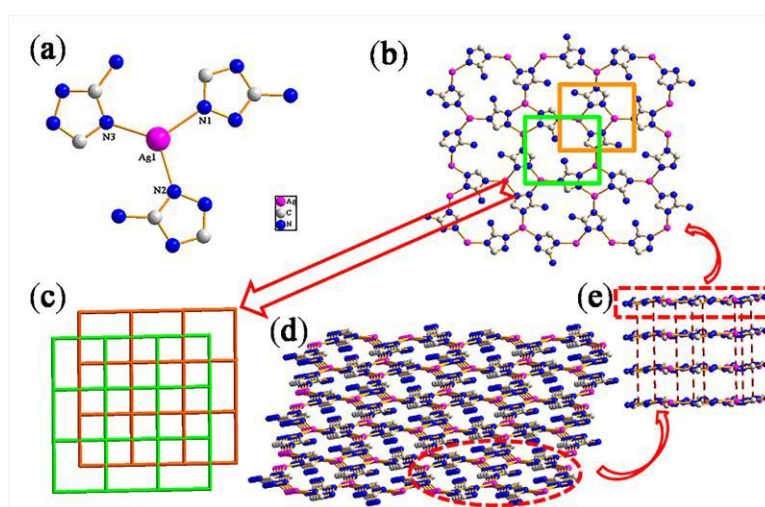


Figure 1. (a) Coordination environments of Ag^{I} in **1**. (b) The 2D planar layer in **1**. (c) Schematic illustrating the 2D topology (the light-green sticks point to six-membered rings and the orange sticks point to sixteen-membered rings). (d, e) The 3D supramolecular framework in **1**. H atoms are omitted for clarity.

Crystal structure of 2: The single crystal X-ray diffraction study determines that compound **2** crystallizes in the monoclinic $P21/c$ space group. Interestingly, the compound **2** is isostructural to **1** (Figure 2a), containing one crystallographically independent Ag^{I} center and one completely deprotonated ntz anion. The obvious difference is that compound **2**, having similar configurations with **1**, yields a teeterboard-like 2D layer (Figure 2e), and the sixteen-membered rings ($\text{Ag}_4\text{N}_8\text{C}_4$) are filled up with two nitro units from two ntz anions (Figure 2b). The corresponding bond distances and angles in **2** are approximately similar as those in **1**. While for **2**, X-ray crystallography analysis shows that the shortest Ag-Ag distance and centroid-centroid distance of

triazole rings between the adjacent layers are the same, 3.6019(8) Å, which is slightly higher than the shortest Ag-Ag distance of **1**, indicating that weak π - π overlap interactions between triazole rings exist in the neighbouring layers (Supporting Information, Figure S3(b)), resulting in a 3D supramolecular framework (Figures 2d and 2e).

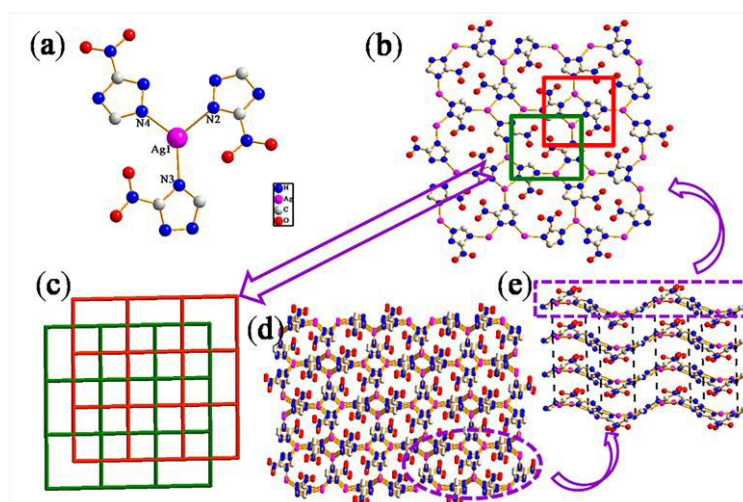


Figure 2. (a) Coordination environments of Ag^I in **2**. (b) The teeterboard-like 2D layer in **2**. (c) Schematic illustrating the 2D topology (the dark-green sticks point to six-membered rings and the red sticks point to sixteen-membered rings). (d, e) The 3D supramolecular framework in **2**. H atoms are omitted for clarity.

Morphologies of 1, 1a, 2 and 2a: In recent years, the tailorability of the shape and size of MOFs has attracted considerable attention originated from their high surface area and widely potential applications in gas adsorption, catalysis and drug release.^[32] In our experiments, we obtained the two compounds in the forms of single crystals (**1** and **2**) and microcrystals (**1a** and **2a**). In order to learn more about the morphologies, we performed scanning electron microscopy (SEM). Figures 3a and 4a show the SEM images of single crystals of compounds **1** and **2**, disclosing that the as-made single crystals with smooth surfaces were bulks with size of about 100 μm for **1** and rods with average length of about 200 μm for **2**. For compound **1**, when increasing the experimental temperature to 140 °C, we obtained microbulk **1a** of 50-100 μm (Figure 3b). On closer inspection, the SEM images obviously record a hierarchical self-assembly process of microplate with thickness of about 2-3 μm (Figures 3c and 3d), which might give a deep visual knowledge of the agglomeration/aggregation mechanism of single crystals. For compound **2**, when the molar ratio

of Ag^{I} and Hntz ligand is 4:4, the nonuniform microrod **2a** with average length in the range of 1-40 μm (Figures 4b, 4c and 4d) could be prepared. Unfortunately, for both **1** and **2**, when the reaction temperature or the amount of reactants was further changed, the same experimental results as **1a** and **2a** were obtained, indicating that reaction temperature is a key factor for the formation of single crystal **1** and the molar ratio of reactants is necessary for the fabrication of single crystal **2**. Thereby, the SEM results might be help to improve the effective utilization of energetic materials by adjusting the size of compounds. XRPD indicated that **1a** and **2a** were crystalline and confirmed the phase purities of the compounds (Supporting Information, Figures S1 and S2).

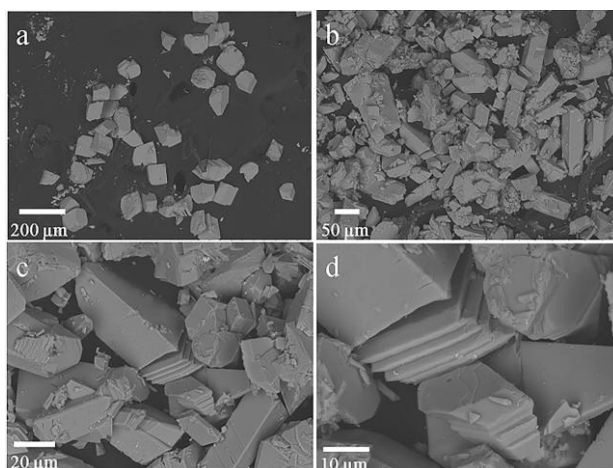


Figure 3. Bulk-like morphologies of $[\text{Ag}(\text{atz})]_n$ containing microbulks obtained at different reaction temperatures.

SEM image (a) of compound **1** in the form of single crystals synthesized at 120 °C. (b, c, d) Microbulks of **1a** synthesized at 140 °C.

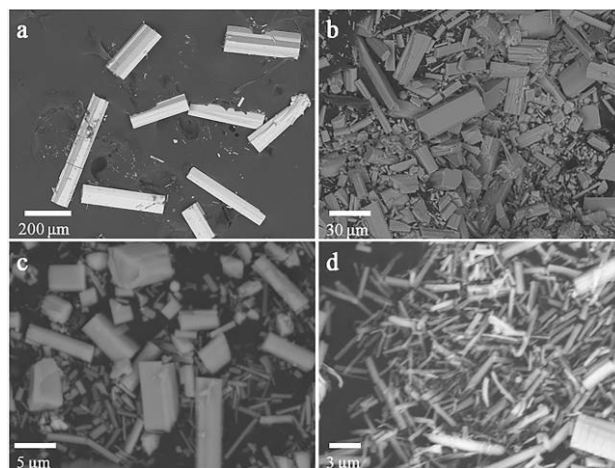


Figure 4. Rod-like morphologies of $[\text{Ag}(\text{ntz})]_n$ containing microrods obtained at different molar ratios of Ag^{I} and Hntz ligand. SEM image (a) Rod-like morphologies of compound **2** synthesized using a molar ratio of Ag^{I} and Hntz of 3:4. (b, c, d) Microrods morphologies of **2a** synthesized using a molar ratio of Ag^{I} and Hntz of 4:4.

Photoluminescence property

Solid-state photoluminescence spectra of the ligands and **1-2** were performed at room temperature. As shown in Figure 5a, upon the optimal excitation at 340 nm, compound **1** represents two significant photoluminescence emission peaks at 497 and 617 nm, and the Stokes shifts are respectively as long as 157 and 277 nm. Based on the previously reported works about the emission of Ag-based compounds,^[27-30] the intense photoluminescence emission at 497 nm may be derived from an intra-ligand $\pi-\pi^*$ transition emission, and the extremely weak one at 617 nm may be tentatively originated to a metal-to-ligand charge transition (MLCT) and/or ligand-to-metal charge transition (LMCT). While compound **2** shows a broad photoluminescence emission peak at 503 nm with the optimal excitation at 384 nm (Figure 5b), and the Stokes shift is about 119 nm resulting from an intra-ligand $\pi-\pi^*$ transition emission. It is significantly worthy to point out that the intense emission peaks slightly blue-shift for **1** and slightly red-shift for **2**, compared with the free ligands at the same excitation, which may be due to the influence of different substituents on ligand (electron-donating group for **1** and electron-withdrawing group for **2**) and the interactions between the substituted ligands and metal ions. In addition, the observed luminescence lifetimes for these emissions of free ligands and **1-2** are only at the nanosecond

ranges (24.18 ns for Hatz ligand, 6.20 ns for **1**, 6.29 ns for Hntz ligand and 8.14 ns for **2**, see Figures. S4-S7 in Supporting Information). The test results may derive from the different substituents on the 1,2,4-triazole and the internal heavy metal effects via d^{10} metal coordination. Therefore, Ag-based compounds containing electron-donating groups/electron-withdrawing groups, might present novel photoluminescence properties.

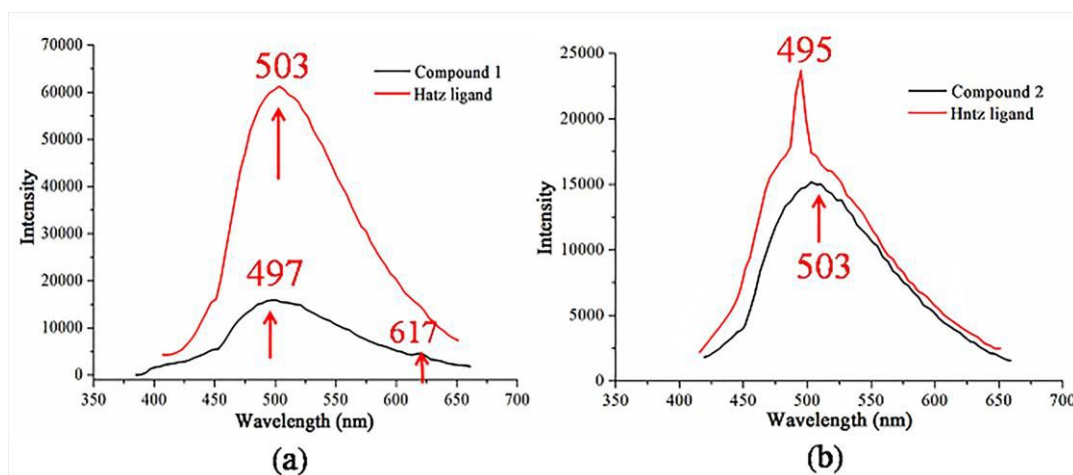


Figure 5. Emission spectra of (a) the ligand Hatz (red line) and compound **1** (black line) at the excitation at 340 nm; (b) the ligand Hntz (red line) and compound **2** (black line) at the excitation at 384 nm in the solid state at room temperature.

Thermal decomposition

To assess the thermal stability of **1** and **2**, DSC and thermogravimetry (TG) analyses were carried out using a linear heating rate of $5\text{ }^{\circ}\text{C min}^{-1}$ at a nitrogen atmosphere (Figure 6). And XRPD experiments were performed to confirm the phase purities of the samples (Figures S1 and S2). The DSC curves reveal that one intense exothermic process, occurs at $360\text{ }^{\circ}\text{C}$ and ends at $385\text{ }^{\circ}\text{C}$ with a peak temperature of $370\text{ }^{\circ}\text{C}$ for **1**. Similarly, the exothermic process of **2** starts at $310\text{ }^{\circ}\text{C}$ and ends at $332\text{ }^{\circ}\text{C}$ with a peak temperature of $325\text{ }^{\circ}\text{C}$. The TG curves suggest that **1** and **2** all undergo one-step weight loss from 348 to $495\text{ }^{\circ}\text{C}$ for **1** and from 305 to $410\text{ }^{\circ}\text{C}$ for **2**, corresponding to the collapse of the main frameworks and the intense exothermic peaks in the DSC curves. These studies show **1** and **2** presented here have a high thermal stability with the decomposition temperatures of $348\text{ }^{\circ}\text{C}$ for **1** and $305\text{ }^{\circ}\text{C}$ for **2**, respectively.

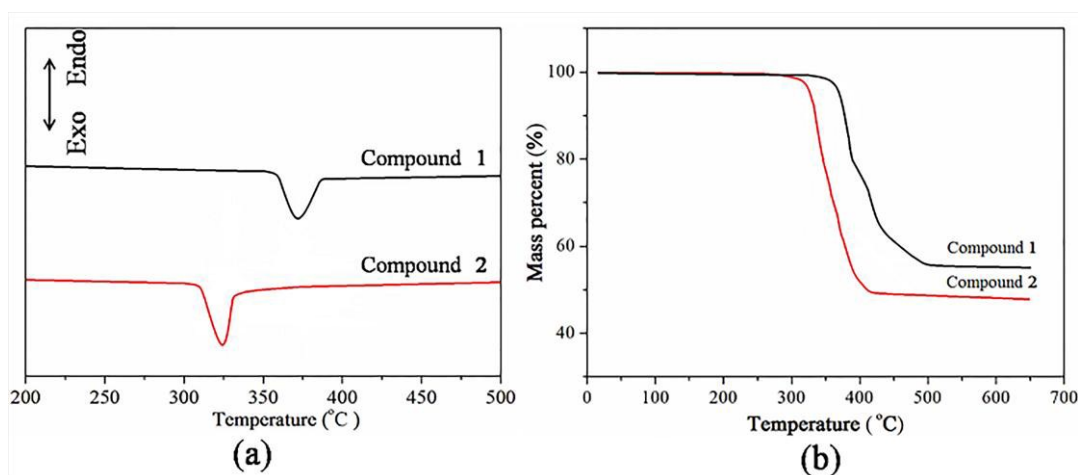


Figure 6. (a) DSC curves and (b) TG curves for **1** and **2**.

Non-isothermal kinetics analysis

In this work, we employed Kissinger's method^[33] and Ozawa-Doyle's method^[34, 35] to perform the apparent activation energy (E) and the pre-exponential factor (A), which could be applied to estimate the thermokinetics stability of **1** and **2**. The Kissinger equations (1) and Ozawa equations (2) are as follows, respectively.

$$\ln\left(\frac{\beta}{T_p^2}\right) = \ln\frac{AR}{E} - \frac{E}{RT_p} \quad (1)$$

$$\log\beta + \frac{0.4567E}{RT_p} = C \quad (2)$$

where T_p is the peak temperature ($^{\circ}\text{C}$); A is the pre-exponential factor (s^{-1}); E is the apparent activation energy (kJ mol^{-1}); R is the gas constant ($8.314 \text{ J mol}^{-1} \text{ K}^{-1}$); β is the linear heating rate ($^{\circ}\text{C min}^{-1}$) and C is a constant.

According to the exothermic peak temperatures measured at four different heating rates of 2, 5, 8 and $10 \text{ }^{\circ}\text{C min}^{-1}$, the thermokinetics parameters of exothermal processes for **1** and **2** were investigated by Kissinger and Ozawa-Doyle methods. The obtained results are showed in Table 1, including the apparent activation energies E_k , and E_o , pre-exponential factor A_k and linear correlation coefficients R_k and R_o .

From Table 1, it is obvious that the exothermic peaks, T_p , shift to higher temperatures as the

heating rate increases and the kinetic parameters for the thermal decomposition reactions of the solid materials are in the normal ranges.^[36, 37] Additionally, the calculated E values using both methods are quite close, and the obtained the values of E_a (the average of E_k and E_o) are 205.845 kJ mol⁻¹ for **1** and 246.395 kJ mol⁻¹ for **2**. Especially, the linear correlation coefficients R are very close to 1 and thus it is proved that the results are extremely credible. On the basis of the calculated values of E_a and $\ln A$, the Arrhenius equations can be expressed as follows: $\ln k = 14.4106 - 205.845 \times 10^3 / (RT)$ for **1**, and $\ln k = 19.5211 - 246.395 \times 10^3 / (RT)$ for **2**, which can be used to estimate the rate constants of the thermal decomposition processes of compounds **1** and **2**.

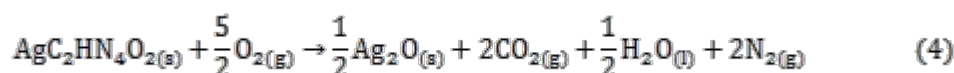
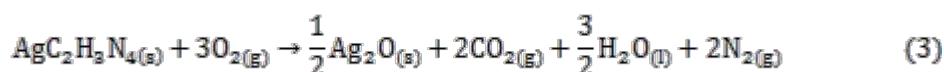
Table 1. The thermokinetics parameters of the exothermic processes at different heating rates.

β (°C min ⁻¹)	Peaks temperatures T_p (°C)	
	1	2
2	355.78	313.10
5	370.36	325.60
8	379.29	328.50
10	379.58	331.40
The calculation results by Kissinger's method E_k (kJ mol ⁻¹)	205.83	247.77
$\ln A$ (s ⁻¹)	14.4106	19.5211
Linear correlation coefficient (R_k)	0.9922	0.9890
The calculation results by Ozawa-Doyle's method E_o (kJ mol ⁻¹)	205.86	245.02
Linear correlation coefficient (R_o)	0.9930	0.9898

Oxygen bomb calorimetry

The constant-volume combustion energies of **1** and **2** were investigated by a precise rotating-oxygen bomb calorimeter (RBC-type II).^[44] Approximately 200 mg of the samples were pressed with a well-define amount of benzoic acid (Calcd. 800 mg) to form a tablet to ensure better combustion. The recorded data are the average of six single measurements. The calorimeter was calibrated by the combustion of certified benzoic acid (Standard Reference Material, 39i, NIST) in an oxygen atmosphere at a pressure of 30.5 bar.

The experimental results for the constant volume combustion energies ($\Delta_c U$) of the energetic compounds **1** and **2** are $(-9488.30 \pm 5.66) \text{ J g}^{-1}$ and $(-7179.32 \pm 6.38) \text{ J g}^{-1}$, respectively. According to the formula $\Delta_c H_m^\theta = \Delta_c U_m^\theta + \Delta nRT$, $\Delta n = n_g(\text{products}) - n_g(\text{reactants})$, (n_g is the total molar amount of gases in the products or reactants, $R = 8.314 \text{ J mol}^{-1} \text{ K}^{-1}$, $T = 298.15 \text{ K}$), the enthalpies of combustion ($\Delta_c H_m^\theta$) can be derived as being $(-1809.31 \pm 1.08) \text{ kJ mol}^{-1}$ for equation (3) and $(-1582.48 \pm 1.41) \text{ kJ mol}^{-1}$ for equation (4). The combustion reaction equations are listed as follows:



$$\Delta_f H_m^\theta(\text{s}) = 0.5\Delta_f H_m^\theta(\text{Ag}_2\text{O}, \text{s}) + 2\Delta_f H_m^\theta(\text{CO}_2, \text{g}) + 1.5\Delta_f H_m^\theta(\text{H}_2\text{O}, \text{l}) - \Delta_c H_m^\theta(\text{1}, \text{s}) \quad (5)$$

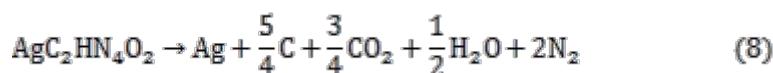
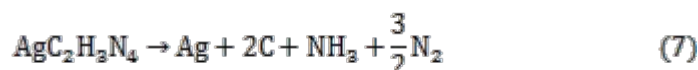
$$\Delta_f H_m^\theta(\text{s}) = 0.5\Delta_f H_m^\theta(\text{Ag}_2\text{O}, \text{s}) + 2\Delta_f H_m^\theta(\text{CO}_2, \text{g}) + 0.5\Delta_f H_m^\theta(\text{H}_2\text{O}, \text{l}) - \Delta_c H_m^\theta(\text{2}, \text{s}) \quad (6)$$

Based on the calculated enthalpies of combustion and known enthalpies of formation of the combustion products^[31, 37] determined experimentally, $\Delta_c H_m^\theta(\text{Ag}_2\text{O}, \text{s}) = (-31) \text{ kJ mol}^{-1}$, $\text{CO}_2(\text{g})$, $\Delta_c H_m^\theta(\text{CO}_2, \text{g}) = (-393.51 \pm 0.13) \text{ kJ mol}^{-1}$, $\text{H}_2\text{O}(\text{l})$, $\Delta_c H_m^\theta(\text{H}_2\text{O}, \text{l}) = (-285.830 \pm 0.040) \text{ kJ mol}^{-1}$, the standard enthalpies of formation of compounds **1** and **2**, $\Delta_c H_m^\theta$, were back-calculated from the combustion equations.^[38] On the basis of Hess's law in thermochemical equations (5)-(6), the standard enthalpies of formation ($\Delta_c H_m^\theta$) of the compounds are calculated as $(578.04 \pm 2.31) \text{ kJ mol}^{-1}$ for **1** and $(637.04 \pm 3.14) \text{ kJ mol}^{-1}$ for **2**, respectively. Notably, compound **2** exhibits a relative high enthalpies of formation compared with **1**, which may be determined by N-O and N=O bonds in the structure of Hntz ligand.

Heat of detonation

In the current work, on the basis of the largest exothermic principle proposed by Kamlet-Jacobs,^[39] we employed a new empirical method previously reported^[31] to investigate the energetic performances of metal-containing explosives without depending on sophisticated computer programs. As in ref. 31, the new and efficient method, which employed the hypothesis of BKW

equation and arbitrary theory of the K-J method, could be applied to perform the detonation performances of metal compounds containing special elements such as Cd and Ag. The detonation reactions estimated by the new methods for **1** and **2** are described by the equations (7) and (8), and heat of detonation values ($Q/J\text{ g}^{-1}$) of **1** and **2** are 3268.05 J g^{-1} and 4865.95 J g^{-1} , respectively.



Detonation property

Detonation properties of **1** and **2** are predicted by key equations as follows, which were concluded by the improved Kamlet-Jacobson (K-J),^[31]

$$D = 1.01(NM^{1/2}Q^{1/2})^{1/2}(1 + 1.30\rho) \quad (9)$$

$$P = 1.55\rho^2NM^{1/2}Q^{1/2} \quad (10)$$

$$Q = \frac{-[\Delta H_f(\text{detonation products}) - \Delta H_f(\text{explosive})]}{\text{formula weight of explosive}} \quad (11)$$

To calculate the detonation velocity ($D/\text{km s}^{-1}$) and detonation pressure (P/GPa) values of **1** and **2**, density ($\rho/\text{g cm}^{-3}$), heat of formation ($\Delta H_f/\text{kJ mol}^{-1}$), heat of detonation ($Q/J\text{ g}^{-1}$), moles of detonation gases per gram of explosive ($N/\text{mol g}^{-1}$), and average molecular weight of gases ($M/\text{g mol}^{-1}$) should first be determined. The complete detonation reactions are described by equations (7) and (8). The D and P values of **1** and **2** are calculated as 6.52 km s^{-1} and 24.07 GPa for **1**, 7.938 km s^{-1} and 36.47 GPa for **2**, respectively.

Sensitivity test

Impact sensitivities are performed by Fall Hammer Apparatus. Twenty milligrams of the compounds are compacted to a copper cap under the press of 39.2 MPa and are hit by 2 kg drop hammer, and the calculated values of h_{50} represent the drop height of 50% initiation probability. Friction sensitivities of **1** and **2** are measured by using a Julius Peter's machine using 20 mg samples. The test results revealed that **1** and **2** did not fire at the highest point of 200 cm corresponding to an impact energy of 40 J , indicating that the compounds are insensitive to impact.

And no friction sensitivity was observed up to 36 kg (360 N). The perfect properties could be comparable to the known explosives such as TNT and energetic MOFs. The results are listed in Table 2.

Table 2. Calculated parameters used in the detonation reactions.

Compounds	$\rho^a/\text{g cm}^{-3}$	$N^b/\%$	$T_{\text{dec}}^{c}/^\circ\text{C}$	$Q^d/\text{kcal g}^{-1}$	$D^e/\text{km s}^{-1}$	P^f/GPa	IS^g/J	FS^h/N
1	2.966	29.33	348	0.781	6.52	24.07	>40	>360
2	3.121	25.35	305	1.163	7.938	36.47	>40	>360
PbHW ^[24]	2.519	39.40	340	1.359	7.715	31.57	>40	>360
PbHWO ^[24]	3.511	27.20	318	0.255	8.122	40.12	>40	>360
HMX ^{[20][38]}	1.950	37.80	280	1.320	8.900	38.39	7.4	—
RDX ^[20]	1.806	37.80	210	1.386	8.600	33.92	7.5	120
TNT ^[20]	1.654	18.50	244	0.897	7.178	20.50	15	353
ATZ-1 ^[23]	1.680	53.35	243	3.618	9.160	35.68	22.5	—
ATZ-2 ^[23]	2.16	43.76	257	1.381	7.773	29.70	30	—
CHP ^[20]	1.948	14.71	194	1.250	8.225	31.73	0.5	—
NHP ^[20]	1.983	33.49	220	1.370	9.184	39.69	—	—
CHHP ^[40]	2.000	23.58	231	0.750	6.205	17.96	0.8	—
ZnHHP ^[40]	2.117	23.61	293	0.700	7.016	23.58	—	—
CoNN-2 ^[41]	1.707	59.85	253	2.658	8.657	32.18	27	>360

^aFrom X-ray diffraction. ^bNitrogen content. ^cDecomposition temperature. ^dThe heat of detonation. ^eDetonation velocity. ^fDetonation pressure. ^gImpact sensitivity. ^hFriction sensitivity. PbTT = lead 3-(tetrazol-5-yl) triazole; PbTTO = lead 3-(tetrazol-5-yl) triazole Oxygen; HMX = Octogen; TNT = Trinitrotoluene; ATZ = 4,4'-azo-1,2,4-triazole; CHP = cobalt hydrazine perchlorate; NHP = nickel hydrazine perchlorate; CHHP = cobalt hydrazine hydrazinecarboxylate perchlorate; ZnHHP = zinc hydrazine hydrazinecarboxylate perchlorate; CoNN = cobalt N,N-bis(1H-tetrazole-5-yl)-amine N,N-bis(1H-tetrazole-5-yl)-amine.

Conclusions

In this study, two isostructural compounds based on Ag^{I} ion and 1,2,4-triazole with NH_2/NO_2 substituents were synthesized and fully characterized by elemental analysis, IR, XPRD, DSC, SEM, and sensitivity tests. Structural analyses show that two compounds **1** and **2** yield

two-dimensional (2D) three-connected layers with a planar layer for **1** and a teeterboard-like layer for **2**. Significantly, we synthesized the two compounds with smaller size by adjusting the reaction conditions and employed SEM to investigate their morphologies, which may be beneficial to control the shape and size of energetic materials. Moreover, photoluminescence spectra reveal that compounds **1** and **2** feature interesting photoluminescence phenomena, namely, the intense emission peaks slightly blue-shift for **1** and slightly red-shift for **2**, which arises from the NH₂/NO₂ substituents on 1,2,4-triazole. Remarkably, **1** and **2** possess excellent insensitivity and thermostability and exhibit high decomposition temperatures of about 348 °C for **1** and 305 °C for **2**, respectively. The densities of **1** and **2** are respectively 2.966 and 3.121 g cm⁻³, and the detonation performances are predicted by a new empirical method without depending on sophisticated computer programs. Compared with TNT and the known energetic metal organic frameworks (MOFs), compound **2** exhibits superior detonation performances: heat of detonation of 1.163 kcal g⁻¹, detonation velocity of 7.938 km s⁻¹ and detonation pressure of 36.47 GPa, which may attribute to the energetic NO₂ substituent. Considering the above, it is worthwhile to further explore the substituent effect of the nitrogen-rich heterocycles on energy performance of energetic MOFs.

Experimental

General caution: Hatz, Hntz and the compounds are potentially hazardous materials, which may tend to explode in certain conditions, and should be treated with great caution. Appropriate safety precautions such as safety glasses and face shields should be taken, especially when the compounds are prepared on a large scale. Only small amounts were used in our present work.

Materials and instruments

All the materials and reagents employed were commercially available and used without further purifications. Elemental analyses (C, H and N) were performed on a Vario EL III analyzer fully automated trace element analyzer and FT-IR spectra were recorded on a Bruker FTIR instrument as KBr pellets. Differential scanning calorimetry (DSC) and thermogravimetric analyses (TGA) were determined by a CDR-4P thermal analyzer of Shanghai Balance Instrument factory and a Netzsch STA 449C instrument, respectively, by using dry oxygen-free nitrogen as the atmosphere, with a flowing rate of 10 mL min⁻¹. About 0.5 mg sample were sealed in aluminum pans in the

temperature range of 25-500 °C for DSC experiments. The morphologies of the samples were observed by scanning electron microscope (SEM, TM3000). The morphology/structure of samples was observed by an FEI Quanta-400 FEG scan electron microscope (FE-SEM) with an accelerating voltage of 20 kV. The sensitivities to impact stimuli were carried out by fall hammer apparatus applying standard staircase method by using a 2 kg drop weight and the results were reported in terms of height for 50% probability of explosion ($h_{50\%}$).^[42] The friction sensitivities were determined on a Julius Peter's apparatus by following the BAM method.^[43] The phase purity of the bulk and powder samples were verified by X-ray powder diffraction (XRPD) measurements carried out on a Rigaku RU200 diffractometer at 60 kV, 300 mA and Cu $K\alpha$ radiation ($\lambda = 1.5406 \text{ \AA}$), with a scan speed of $5 \text{ }^\circ\text{min}^{-1}$ and a step size of 0.02 ° in 2θ . Densities of two compounds **1** and **2** were measured by using Automatic Density Analyzer, ULTRAPYC 1200e. The constant-volume combustion energies of the compounds were determined by a precise rotating-bomb calorimeter (RBC-type II).^[44] Solid-state photoluminescence spectra and lifetime measurements were carried out at room temperature with an Edinburgh FL-FS90 TCSPC system.

Synthetic procedures

[Ag(atz)]_n (1). Compound **1** was prepared from a mixture of Hatz (0.4 mmol) in distilled water (3 ml) and AgNO₃ (0.3 mmol) in acetonitrile (MeCN, 3 ml), which was then added to an aqueous solution (2 ml) of NaN₃ (0.4 mmol). After stirring for 30 min in air, the pH value was adjusted to 3 by the addition of dilute nitric acid solution. The resulting mixture was sealed in a 25 mL Teflon-lined stainless steel autoclave and heated to 120 °C for 72 h under autogenous pressure, and then cooled to room temperature at a rate of $5 \text{ }^\circ\text{C h}^{-1}$. The colorless bulk-like crystals of **1** were collected by filtration, washed with water and dried in air (Yield: 67% based on Ag). Elem anal. Calcd (%) for AgC₂H₃N₄ (190.95): C, 12.57; H, 1.57; N, 29.33. Found: C, 12.54; H, 1.62; N, 29.35. IR (KBr, cm⁻¹): 3433s, 2987w, 2938m, 2845m, 2604w, 2486m, 2361w, 2215w, 1637s, 1505s, 1435m, 1386s, 1233s, 1143m, 1031m, 884w, 791w, 713w, 696m, 479w.

[Ag(atz)]_n (1a). An identical procedure with **1** was followed to prepare **1a** except the maintained temperature was increased to 140 °C for 72 h. The colorless bulk-like microcrystals of **1a** were obtained by filtration, washed with water and dried in air (Yield: 69% based on Ag). Elem anal. Calcd (%) for AgC₂H₃N₄ (190.95): C, 12.57; H, 1.57; N, 29.33. Found: C, 12.54; H, 1.63; N, 29.36. IR (KBr, cm⁻¹): 3433s, 2987w, 2938m, 2845m, 2604w, 2486m, 2361w, 2215w, 1637s,

1505s, 1435m, 1386s, 1233s, 1143m, 1031m, 884w, 791w, 713w, 696m, 479w.

[Ag(ntz)]_n (2). A mixture of AgNO₃ (0.4 mmol), Hntz (0.3 mmol) and water (8 ml) was stirred under air atmosphere until complete dissolution of all components, and then transferred and sealed into a 25 mL Teflon-lined stainless steel autoclave. The reaction system was heated up to 100 °C for 72 h under autogenous pressure, and then cooled to room temperature at a rate of 5 °C h⁻¹. The pale yellow rod-like crystals of **2** were collected by filtration, washed with water and dried in air (Yield: 59% based on Ag). Elem anal. Calcd (%) for AgC₂HN₄O₂ (220.94): C, 10.86; H, 0.45; N, 25.35. Found: C, 10.83; H, 0.46; N, 25.37. IR (KBr, cm⁻¹): 3428s, 3130m, 2921w, 2684w, 2650w, 2413w, 2230w, 1790w, 1635m, 1554s, 1493s, 1401s, 1362s, 1296s, 1257m, 1169s, 1062s, 984m, 896m, 837s, 655s, 553w.

[Ag(ntz)]_n (2a). The same synthetic route as that for **2** was used except that 0.3 mmol Hntz was replaced by 0.4 mmol Hntz. The pale yellow rod-like microcrystals of **2a** were collected by filtration, washed with water and dried in air (Yield: 63% based on Ag). Elem anal. Calcd (%) for AgC₂HN₄O₂ (220.94): C, 10.86; H, 0.45; N, 25.35. Found: C, 10.78; H, 0.47; N, 25.39. IR (KBr, cm⁻¹): 3428s, 3130m, 2921w, 2684w, 2650w, 2413w, 2230w, 1790w, 1635m, 1554s, 1493s, 1401s, 1362s, 1296s, 1257m, 1169s, 1062s, 984m, 896m, 837s, 655s, 553w.

X-ray crystallography

Crystallographic data of compounds **1** and **2** were collected on a Bruker Smart Apex CCD diffractometer equipped with graphite monochromatized Mo K α radiation ($\lambda = 0.71073 \text{ \AA}$) using ω and ϕ scan mode. The single-crystal structures of two compounds **1** and **2** were solved by direct methods using SHELXS-97,^[45] and refined by means of full-matrix least-squares procedures on F^2 with SHELXL-97^[46] crystallographic program. All non-H atoms were located using subsequent Fourier-difference methods and refined anisotropically. In all cases, hydrogen atoms were placed in calculated positions and thereafter allowed to ride on their parent atoms. The crystal data and structure refinement details of compounds are summarized in Table 3, while the selected bond lengths and angles data are presented in Table S1 and S2. The crystal structures have been deposited in the Cambridge Crystallographic Data Centre, with CCDC 1057778 for **1** and 1059721 for **2**, respectively. These data can be obtained free of charge from The Cambridge Crystallographic Data Centre via www.ccdc.cam.ac.uk/data_request/cif.

Table 3. Crystallographic data for compounds **1** and **2**.

	1	2
Empirical formula	AgC ₂ H ₃ N ₄	AgC ₂ HN ₄ O ₂
Formula weight	190.95	220.94
Crystal system	Monoclinic	Monoclinic
space group	<i>C</i> 2/ <i>c</i>	<i>P</i> 21/ <i>c</i>
<i>a</i> (Å)	10.0809(19)	3.6019(7)
<i>b</i> (Å)	11.449(2)	11.273(2)
<i>c</i> (Å)	7.5369(15)	11.600(2)
α (°)	90	90
β (°)	100.493(3)	93.389(3)
γ (°)	90	90
<i>V</i> (Å ³)	855.3(3)	470.16(16)
<i>Z</i>	8	4
<i>D_c</i> (g cm ⁻³)	2.966	3.121
<i>T</i> (K)	296(2)	296(2)
μ (mm ⁻¹)	4.549	4.192
<i>F</i> (000)	720	416
Reflections collected/unique	2308 / 905	2084 / 832
<i>R</i> (int)	0.0188	0.0312
Data/restraints/parameters	905/2/72	832 / 0 / 83
GOF ^c on <i>F</i> ²	0.913	1.059
<i>R</i> ₁ ^a [<i>I</i> > 2σ(<i>I</i>)]	0.0315	0.0244
<i>wR</i> ₂ ^b (all data)	0.1121	0.0580

^a $R_1 = \sum ||F_o| - |F_c|| / \sum |F_o|$; ^b $wR_2 = [\sum w(F_o^2 - F_c^2)^2 / \sum w(F_o^2)^2]^{1/2}$.

^c GOF = goodness of fit.

Acknowledgements

This work was financially supported by the National Natural Science Foundation of China (Grant Nos. 21373162, 21203149, 21473135 and 21173168) and the Nature Science Foundation of Shanxi Province (Grant Nos. 11JS110, FF10091 and SJ08B09).

Supporting Information:

Electronic Supplementary Information (ESI) available: The CIF files give crystallographic data for compounds **1** and **2**. Figures S1-S7 and Tables S1-S2 see supporting information.

References

- 1 H.-X. Gao and J. M. Shreeve, *Chem. Rev.*, 2011, **111**, 7377.
- 2 V. Thottampudi, T. K. Kim, K. H. Chung and J. S. Kim, *Bull. Korean Chem. Soc.*, 2009, **30**, 2152-2154.
- 3 G. Singh and S. P. Felix, *J. Hazard. Mater.*, 2002, **90**, 1-17.
- 4 M. Göbel, K. Karaghiosoff and T. M. Klapötke, *Angew. Chem. Int. Ed.*, 2006, **45**, 6037.
- 5 R.-H. Wang, H.-Y. Xu, Y. Guo, R.-J. Sa and J. M. Shreeve, *J. Am. Chem. Soc.*, 2010, **132**, 11904-11905.
- 6 Y. Guo, H. Gao, B. Twamley and J. M. Shreeve, *Adv. Mater.*, 2007, **19**, 2884.
- 7 Q.-H. Zhang and J. M. Shreeve, *Angew. Chem. Int. Ed.*, 2014, **53**, 2540-2542.
- 8 N. Fischer, D. Izsák, T. M. Klapötke, S. Rappenglück and J. Stierstorfer, *Chem.-Eur. J.*, 2012, **18**, 4051-4062.
- 9 G. Fischer, G. Holl, T.M. Klapötke and J. J. Weigand, *Thermochim. Acta.*, 2005, **437**, 168.
- 10 S. Huber, D. Izsak, K. Karaghiosoff, T. M. Klapötke and S. Reuter, *Propellants, Explos., Pyrotech.*, 2010, **35**, 1-9.
- 11 P.-P. Liu, A.-L. Cheng, Q. Yue, N. Liu, W.-W. Sun, and E.-Q. Gao, *Cryst. Growth Des.*, 2008, **8**, 1668-1674.
- 12 Y.-X. Guo, X. Feng, T.-H Han, S. Wang, Z.-G Lin, Y.-P Dong, and B. Wang, *J. Am. Chem. Soc.*, 2014, **136**, 15485-15488.
- 13 K. Karaghiosoff, T. M. Klapötke, A. N. Michailovski, H. Nöth, M. Suter and G. Holl, *Propellants Explos. Pyrotech.*, 2003, **28**, 1-6.

- 14 R. W. Millar, S. P. Philbin, R. P. Claridge and J. Hamid, *Propellants, Explos., Pyrotech.*, 2004, **29**, 81-92.
- 15 M.-X. Zhang, P. E. Eaton and R. Gilardi, *Angew. Chem. Int. Ed.*, 2000, **39**, 401-404.
- 16 J. Köhler and J. Meyer, *Explosivstoffe*, 9th ed, Wiley-VCH, D-Weinheim, 1998, 174.
- 17 T. M. Willey, T. van Buuren, J. R. Lee, G. E. Overturf, J. H. Kinney, J. Handly, B. L. Weeks and J. Ilavsky, *Propellants, Explos., Pyrotech.*, 2006, **31**, 466-471.
- 18 (a) S. Noro, S. Kitagawa, M. Kondo and K. Seki, *Angew. Chem. Int. Ed.*, 2000, **112**, 2161-2164; (b) S.-N. Wang, H. Xing, Y.-Z. Li, J.-F. Bai, M. Scheer, Y. Pan and X.-Z. You, *Chem. Commun.*, 2007, 2293-2295; (c) C. A. Bauer, T. V. Timofeeva, T. B. Settersten, B. D. Patterson, V.-H. Liu, B. A. Simmons and M. D. Allendorf, *J. Am. Chem. Soc.*, 2007, **129**, 7136-7144; (d) Y.-C. Shen, Z.-Y. Li, L.-H. Wang, Y.-X. Ye, Q. Liu, X.-L. Ma, Q.-H. Chen, Z.-J. Zhang and S.-C. Xiang, *J. Mater. Chem. A*, 2015, **3**, 593-599; (e) Z.-J. Zhang, Z.-Z. Yao, S.-C. Xiang and B.-L. Chen, *Energy Environ. Sci.*, 2014, **7**, 2868-2899; (f) Y. Chen, Z.-Y. Li, Q. Liu, Y.-C. Shen, X.-Z. Wu, D.-D. Xu, X.-L. Ma, L.-H. Wang, Q.-H. Chen, Z.-J. Zhang and S.-C. Xiang, *Cryst. Growth Des.*, DOI: 10.1021/acs.cgd.5b00473.
- 19 (a) B. Moulton and M. J. Zaworotko, *Chem. Rev.*, 2001, **101**, 1629-1658; (b) H. Reinsch, M. A. van der Veen, B. Gil, B. Marszalek, T. Verbiest, D. de Vos and N. Stock, *Chem. Mater.*, 2012, **25**, 17-26; (c) S. M. Kuznicki, V. A. Bell, S. Nair, H. W. Hillhouse, R. M. Jacubinas, C. M. Braunbarth, B. H. Toby and M. Tsapatsis, *Nature*, 2001, **412**, 720-724.
- 20 O. S. Bushuyev, P. Brown, A. Maiti, R. H. Gee, G. R. Peterson, B. L. Weeks and L. J. Hope-Weeks, *J. Am. Chem. Soc.*, 2012, **134**, 1422.
- 21 R. P. Singh, R. D. Verma, D. T. Meshri and J. M. Shreeve, *Angew. Chem. Int. Ed.*, 2006, **45**, 3584-3601.
- 22 G.-H. Tao, D. A. Parrish and J. M. Shreeve, *Inorg. Chem.*, 2012, **51**, 5305-5312.
- 23 S.-H. Li, Y. Wang, C. Qi, X.-X. Zhao, J.-C. Zhang, S.-W. Zhang and S.-P. Pang, *Angew. Chem., Int. Ed.*, 2013, **52**, 14031-14035.
- 24 W.-J. Gao, X.-Y. Liu, Z.-Y. Su, S. Zhang, Q. Yang, Q. Wei, S.-P. Chen, G. Xie, X.-W. Yang and S.-L. Gao, *J. Mater. Chem. A.*, 2014, **2**, 11958-11965.
- 25 J. Evers, I. Gospodinov, M. Joas, T. M. Klapötke and J. Stierstorfer, *Inorg. Chem.*, 2014, **53**, 11749-11756.

- 26 P. J. Steel and C. M. Fitchett, *Coord. Chem. Rev.*, 2008, **252**, 990.
- 27 Q. Zhang, D. Chen, X. He, S.-L. Huang, J.-L. Huang, X.-Q. Zhou, Z.-W. Yang, J.-S. Li, H.-Z. Li and F. Nie, *CrystEngComm.*, 2014, **16**, 10485-10491.
- 28 M. A. Omary, M. A. Rawashdeh-Omary, H. V. Diyabalanage and H. R. Dias, *Inorg. Chem.*, 2003, **42**, 8612-8614.
- 29 J.-P. Zhang, Y.-Y. Lin, W.-X. Zhang and X.-M. Chen, *J. Am. Chem. Soc.*, 2005, **127**, 14162-14163.
- 30 (a) Q.-G. Zhai, X.-Y. Wu, S.-M. Chen, Z.-G. Zhao and C.-Z. Lu, (2007). *Inorg. Chem.*, 2007, **46**, 5046-5058; (b) J.-P. Zhang, Y.-Y. Lin, X.-C. Huang and X.-M. Chen, *J. Am. Chem. Soc.*, 2005, **127**, 5495-5506; (c) M.-L. Tong, X.-M. Chen, B.-H. Ye, and L.-N. Ji, *Angew. Chem. Int. Ed.*, 1999, **38**, 2237-2240.
- 31 (a) Y. Wang, J.-C. Zhang, H. Su, S.-H. Li, S.-W. Zhang and S.-P. Pang, *J. Mater. Chem. A.*, 2014, **118**, 4575-4581; (b) A. Bondi, *J. Phys. Chem.*, 1964, **68**, 441-451.
- 32 (a) Q. Liu, L.-N. Jin and W.-Y. Sun, *CrystEngComm.*, 2013, **15**, 8250-8254; (b) D. Zacher, O. Shekhah, C. Wöll and R. A. Fischer, *Chem. Soc. Rev.*, 2009, **38**, 1418-1429; (c) A. U. Czaja, N. Trukhan and U. Müllerb, *Chem. Soc. Rev.*, 2009, **38**, 1284-1293; (d) A. M. Spokoyny, D. Kim, A. Sumrein and C. A. Mirkin, *Chem. Soc. Rev.*, 2009, **38**, 1218-1227; (e) Q. Liu, L.-N. Jin and W.-Y. Sun, *Chem. Commun.*, 2012, **48**, 8814-8816.
- 33 H. E. Kissinger, *Anal. Chem.*, 1957, **29**, 1702-1706.
- 34 T. Ozawa, *Bull. Chem. Soc. Jpn.*, 1965, **38**, 1881-1886.
- 35 C. Doyle, Kinetic analysis of thermo-gravimetric data, *J. Appl. Polym. Sci.*, 1961, **5**, 285-292.
- 36 R.-Z. Hu, Z.-Q. Yang and Y.-J. Liang, *Thermochim. Acta.*, 1988, **123**, 135-151.
- 37 J. D. Cox, D. D. Wagman and V. A. Medvedev, CODATA Key Values for Thermodynamics. Hemisphere Publishing Corp: New York, 1989.
- 38 Y. Wang, L. Gong, Y.-B. Li and Z.-X. Wei, *Chin. J. Chem. Eng.*, 2010, **18**, 397-401.
- 39 M. J. Kamlet and S. Jacobs, *J. Chem. Phys.*, 2003, **48**, 23-35.
- 40 O. S. Bushuyev, G. R. Peterson, P. Brown, A. Maiti, R. H. Gee, B. L. Weeks and L. J. Hope-Weeks, *Chem.-Eur. J.*, 2013, **19**, 1706-1711.
- 41 S. Zhang, X.-Y. Liu, Q. Yang, Z.-Y. Su, W.-J. Gao, Q. Wei, G. Xie, S.-P. Chen and S.-L. Gao, *Chem.-Eur. J.*, 2014, **20**, 7906-7910.

- 42 R. Meyer and J. Köhler (Eds.), *Explosives*, 4th ed. revised and extended, VCH Publishers, New York, 1993, 149.
- 43 R. Meyer and J. Köhler (Eds.), *Explosives*, 4th ed. revised and extended, VCH Publishers, New York, 1993, 197.
- 44 X. Yang, S. Chen, S. Gao, H. Li and Q. Shi, *Instrum Sci. Technol.*, 2002, **30**, 311-321.
- 45 G. M. Sheldrick, *SHELXS-97*, Program for X-ray Crystal Structure Determination, University of Göttingen, Germany, 1997.
- 46 G. M. Sheldrick, *SHELXL-97*, Program for X-ray Crystal Structure Refinement, University of Göttingen, Germany, 1997.